

Pathogenic soluble tau peptide disrupts endothelial calcium signaling and vasodilation in the brain microvasculature

Journal of Cerebral Blood Flow & Metabolism
0(0) 1–9
© The Author(s) 2024
Article reuse guidelines:
sagepub.com/journals-permissions
DOI: 10.1177/0271678X241235790
journals.sagepub.com/home/jcbfm



Amreen Mughal^{1,*†}, Adrian M Sackheim^{2,*}, Masayo Koide¹, Grace Bonson², Grace Ebner¹, Grant Hennig¹, Warren Lockette³, Mark T Nelson^{1,4} and Kaley Freeman^{1,2}

Abstract

The accumulation of the microtubule-associated tau protein in and around blood vessels contributes to brain microvascular dysfunction through mechanisms that are incompletely understood. Delivery of nutrients to active neurons in the brain relies on capillary calcium (Ca^{2+}) signals to direct blood flow. The initiation and amplification of endothelial cell Ca^{2+} signals require an intact microtubule cytoskeleton. Since tau accumulation in endothelial cells disrupts native microtubule stability, we reasoned that tau-induced microtubule destabilization would impair endothelial Ca^{2+} signaling. We tested the hypothesis that tau disrupts the regulation of local cerebral blood flow by reducing endothelial cell Ca^{2+} signals and endothelial-dependent vasodilation. We used a pathogenic soluble tau peptide (T-peptide) model of tau aggregation and mice with genetically encoded endothelial Ca^{2+} sensors to measure cerebrovascular endothelial responses to tau exposure. T-peptide significantly attenuated endothelial Ca^{2+} activity and cortical capillary blood flow *in vivo*. Further, T-peptide application constricted pressurized cerebral arteries and inhibited endothelium-dependent vasodilation. This study demonstrates that pathogenic tau alters cerebrovascular function through direct attenuation of endothelial Ca^{2+} signaling and endothelium-dependent vasodilation.

Keywords

Alzheimer's disease, dementia, endothelium, calcium, cerebral blood flow

Received 11 September 2023; Revised 3 January 2024; Accepted 27 January 2024

Introduction

Impaired cerebral blood flow plays a crucial role in the development of degenerative neurological diseases such as Alzheimer's disease (AD) and Chronic Traumatic Encephalopathy (CTE). Both AD and CTE are characterized by accumulation of hyperphosphorylated forms of the microtubule-associated protein tau around blood vessels.^{1–5} Tau disrupts cerebral blood flow regulation, but mechanisms are incompletely understood.^{6,7} The precise and efficient delivery of nutrients to active neurons in the brain relies on the intricate network of capillaries in which local inositol 1,4,5-triphosphate IP_3 receptor (IP_3R)–mediated calcium (Ca^{2+}) signals through nitric oxide production direct blood flow.⁸ These events range from small, brief proto-events, which represent the release of Ca^{2+} through a single IP_3R channel, to larger,

¹Department of Pharmacology, University of Vermont, Burlington, VT, USA

²Department of Emergency Medicine, University of Vermont, Burlington, VT, USA

³Division of Endocrinology, Wayne State University School of Medicine, Detroit, MI, USA

⁴Division of Cardiovascular Sciences, University of Manchester, Manchester, UK

*Equal contribution.

†Current address: The Neurovascular Research Unit- Stroke Branch, National Institute of Neurological Disorders and Stroke, National Institutes of Health, Bethesda, MD, USA.

Corresponding author:

Kaley Freeman, Department of Emergency Medicine, University of Vermont, Firestone Medical Research Building 452, 149 Beaumont Avenue, Burlington VT 05405-0068, USA.
Email: kaley.freeman@uvm.edu

sustained compound events lasting up to approximately one minute, involving clusters of channels.⁸ As a result, intracellular Ca^{2+} activates nitric oxide synthesis, which enhances local blood flow to active neurons.⁸

It was recently demonstrated that brain microvascular endothelial cells internalize soluble tau oligomers in pathological conditions through a process that depends on heparan sulfate proteoglycans.⁷ Endothelial cell internalization of soluble tau triggers phosphorylation of endogenous tau at threonine 231, which promotes destabilization of microtubules and reduces microtubule density.⁷ This has important implications, because microtubule function is required for IP_3R clustering and Ca^{2+} signaling in endothelial cells. Prior work has shown that perturbation of the microtubule cytoskeleton by the drugs colchicine and colcemid prevents the initiation of IP_3 -evoked Ca^{2+} signals in endothelial cells.^{9,10} Furthermore, disruption of microtubules with nocodazole impairs the microtubule-facilitated motility of IP_3Rs , preventing the localization of the channel which is needed for efficient and graded recruitment of channels with increasing stimulus strength.¹¹ Microtubules also have direct interactions with the consensus motif for EB binding (TxIP) of IP_3Rs through the microtubule end-binding protein 3 (EB3); depletion or deletion of EB3, or mutation of the TxIP motif on IP_3Rs , prevents clustering and functional coupling between IP_3Rs .¹² Since tau accumulation in endothelial cells disrupts native microtubule stability, we reasoned that tau-induced endothelial microtubule destabilization would impair endothelial Ca^{2+} signaling.

Here, we tested the hypothesis that tau aggregates impair the regulation of regional cerebral blood flow by acutely reducing endothelial cell Ca^{2+} signals and disrupting endothelium-dependent vasodilation. We used a soluble pathogenic tau peptide (T-peptide) model of tau aggregation. This cell-permeable hexameric peptide derived from the third microtubule-binding repeat of tau self-assembles *in vitro* into paired helical filament-like aggregates providing an established paradigm for studying mechanisms underlying tauopathy.^{13,14} To isolate and measure Ca^{2+} activity from endothelial cells, we studied mice with endothelial-specific expression of the Ca^{2+} biosensor GCaMP8 driven by the cadherin 5 promoter (*Cdh5-GCaMP8*).⁸ We utilized two-photon laser scanning microscopy via an acute cranial window to record microvascular endothelial Ca^{2+} signals *in vivo*; the addition of intravenous fluorescent-dextran allowed measurement of regional cerebral blood flow. We also isolated small cerebral arteries to study direct vascular effects of T-peptide with pressure myography. Together, these experiments demonstrate that T-peptide has rapid and direct effects on brain microvascular endothelium, reducing Ca^{2+}

signaling and impairing the regional regulation of cerebral blood flow.

Methods

Animals

Male C57BL/6J mice (Jackson Laboratories, Bar Harbor, ME), aged 8–12 weeks, were assigned at random to either experimental or control treatment groups for *in vivo* cerebral hemodynamics measurements and ex-vivo pressure myography. *Cdh5-GCaMP8* mice (male, age 8–12 weeks) were used for *in vivo* Ca^{2+} imaging studies. Mice were kept on a 12 h light/dark cycle, with *ad libitum* access to food and water and were housed in groups of five. All studies were conducted in accordance with the Guidelines for the Care and Use of Laboratory Animals (National Institute of Health), Guidelines for Survival Rodent Surgery (National Institute of Health) and approved by the Institutional Animal Care and Use Committee of the University of Vermont. All procedures were conducted and reported in accordance with the ARRIVE guidelines (Animal Research: Reporting In Vivo Experiments) (<https://www.nc3rs.org.uk/arrive-guidelines>).

In vivo imaging of cerebral hemodynamics

Mice were anesthetized with isoflurane (5% induction; 2% maintenance). The skull was exposed, a stainless-steel head plate was attached, and a small circular cranial window was created over the somatosensory cortex. Approximately 150 μL of a 3-mg/mL solution of fluorescein isothiocyanate (FITC)- or tetramethylrhodamine isothiocyanate (TRITC)-dextran (MW 150 kDa) in sterile saline was injected intravenously into the retro-orbital sinus to allow visualization of the cerebral vasculature and contrast imaging of red blood cells (RBCs). Upon conclusion of surgery, isoflurane anesthesia was replaced with α -chloralose (50 mg/kg) and urethane (750 mg/kg). Body temperature was maintained at 37 °C throughout the experiment using an electric heating pad. The brain was continuously perfused with artificial cerebrospinal fluid (aCSF) containing (in mM): 124 NaCl, 3 KCl, 2 CaCl_2 , 2 MgCl_2 , 1.25 NaH_2PO_4 , 26 NaHCO_3 , and 4 glucose (pH 7.4).

Calcium imaging. The *Cdh5-GCaMP8* mice used in these experiments allowed direct visualization of capillary endothelial cell-specific calcium signals in cortical capillaries, with single-plane imaging in a 425 μm × 425 μm field of view (FOV) at ~2.5 Hz through a cranial window as previously described.⁸ Baseline capillary endothelial cells Ca^{2+} activity was recorded in a

FOV for approximately 360 seconds. Then, T-peptide (100 nM) was applied directly to the surface of the brain exposed by the cranial window and allowed to equilibrate for approximately 20 minutes to allow for penetration of T-peptide. An additional 360 second recording in the same FOV was then performed, allowing us to compare capillary endothelial cell Ca^{2+} activity before and after cortical application of T-peptide.

RBC flux measurements. These experiments were performed as previously described.⁸ Briefly, a micropipette was introduced into the cortex and maneuvered adjacent to the capillary region (3rd–4th order branches) under study (R1). A pressurized brief injection (7 ± 1 PSI for 300 ms) of 100 nM T-peptide (Tocris, USA) with TRITC-dextran (MW 150 kDa; 0.06 mg/mL) was ejected directly onto the capillary. This approach restricted T-peptide delivery to the target capillary (R1) and caused minimal displacement of the surrounding tissue. RBC flux data was collected by line scanning the capillary in the region of interest (R1) at 5 kHz. In additional experiments, line scans were performed from other capillaries (R2) in the same field of view, which were approximately ~ 70 – $100 \mu\text{m}$ away from, but connected with, the target capillary (R1). Continuous recordings of RBC flux from each line scan were obtained for 6 seconds at baseline followed by approximately 5 minutes after T-peptide application. Three dimensional vascular maps were created in the same fields using the same $425 \mu\text{m} \times 425 \mu\text{m}$ dimensions in the x-y axes across $\sim 300 \mu\text{m}$ in the z-axis (with $2 \mu\text{m}$ spacing between the planes) for identifying capillary branch order and connectivity of the capillary network. Images were acquired through a Zeiss $20\times$ Plan Apochromat 1.0 NA DIC VIS-IR water-immersion objective mounted on a Zeiss LSM-7 multiphoton microscope (Zeiss, USA) coupled to a Coherent Chameleon Vision II Titanium-Sapphire pulsed infrared laser (Coherent, USA). GCaMP8 and FITC/TRITC-dextran were excited at 920 nm and 820 nm respectively, and emitted fluorescence was separated through 500- to 550- and 570- to 610-nm band-pass filters, respectively.

Ex vivo pressure myography

Cerebral vessels were harvested and pressurized in a myograph system as previously described.¹⁵ Briefly, mice were euthanized and a full craniectomy was performed to expose the brain, which was then dissected and placed into cold (4°C) HEPES-buffered physiological saline solution (HEPES-PSS) with the following composition (in mM): 134 NaCl, 6 KCl, 2 mM CaCl_2 , 1 MgCl_2 , and 7 glucose (pH 7.4). The posterior cerebral artery (PCA) was then excised and cannulated in

a pressure myograph chamber (Living Systems Instrumentation, USA) as previously described.¹⁵ Briefly, arteries were maintained in aCSF solution at 37°C and allowed to equilibrate for 10 minutes at 10 mm Hg before experimentation. Intraluminal pressure was controlled using a pressure servo system (Living Systems Instrumentation, USA) and blood vessel diameters were continuously recorded using edge-detection software (IonOptix, USA). Intraluminal pressure was increased to 80 mm Hg and vessels were allowed to develop spontaneous myogenic tone. Endothelial viability was tested using $1 \mu\text{M}$ NS309 (Cayman Chemical, USA) and a dilatory response $>85\%$ was considered “intact.” Experimental interventions were then carried out using T-peptide (20 minutes; 100 nM), bradykinin ($10 \mu\text{M}$; Cayman Chemical, USA), NS309 ($1 \mu\text{M}$), or spermine NONOate (1 – 100 nM ; Cayman Chemical, USA). The bath solution was then exchanged with 0-Ca^{2+} saline solution with $100 \mu\text{M}$ diltiazem (Sigma-Aldrich, USA) to elicit maximal passive diameter. The percentage change in diameter to pharmacological intervention was measured at the point of peak dilation or constriction and calculated as: change in diameter (%) = [(diameter after drug administration – baseline diameter)/(passive diameter – baseline diameter) $\times 100$].

Data analysis & statistics

GraphPad Prism software (ver. 9.4.1; GraphPad Software, USA) was used for x–y graphing and analysis; values are presented as means \pm standard deviation (SD). Data were tested for normality and appropriate parametric or non-parametric statistical tests were subsequently applied. Differences were considered significant if $P < 0.05$. RBC flux was analyzed offline using custom software (SparkAn, Adrian Bonev, University of Vermont, USA). Flux data were binned at 1 second intervals. Mean baseline flux data for summary figures were obtained by averaging the baseline (6 seconds) for each measurement before pressure ejection of 100 nM T-peptide. The peak response was defined as the peak 1-second flux bin after delivery of T-peptide within the remaining scanning (240–300 seconds). The depth of capillaries below the surface was estimated from z-stack series acquired before pipette placement. To avoid limitations of standard F/F_0 methods and accurately characterize and analyze Ca^{2+} events in brain capillaries, we used our custom autonomous image analysis program ‘VolumetryG9’.⁸ This method uses signal-to-noise ratios and statistical z-scores (Z_{scr}) combined with spatiotemporal (ST) mapping to accurately quantify the full dimensional characteristics of Ca^{2+} events, combining amplitude (Z_{scr}), size (μm) and duration (s) as the conglomerate variable ZUMS

(Zscr- $\mu\text{m}\cdot\text{second}$).⁸ Each animal or vessel served as its own control and experiments were analyzed in a pairwise fashion; therefore, anonymizing was not feasible. Sample sizes for all experimental preparations were estimated using our previous experience.¹⁶

Results

Cortical capillary blood flow and EC Ca^{2+} signaling are significantly reduced by T-peptide *in vivo*

Targeted delivery of nutrients to active neurons in the brain depends on capillary endothelial cell Ca^{2+} signals. Since tau accumulation in microvascular brain endothelial cells disrupts the native microtubule function,⁷ and these microtubules are needed for initiation and amplification of Ca^{2+} signals, we postulated that tau exposure would lead to a rapid reduction in endothelial Ca^{2+} signaling. To test this hypothesis, we leveraged our recently developed *Cdh5*-GCaMP8

transgenic mice that express the Ca^{2+} indicator, GCaMP8, under the transcriptional control of the *Cdh5* (cadherin 5) promoter for targeted expression in vascular endothelial cells.⁸ We also injected TRITC-dextran in these mice to visualize brain capillaries, which provided a map of the cortical vasculature using 3-dimensional z-stacks in a $425 \times 425 \mu\text{m}$ FOV. We defined capillaries as vessels located between penetrating arterioles and ascending venules and assigned them branch orders as previously described.^{8,17} We then recorded the capillary endothelial cells (cECs) Ca^{2+} activity in layer II-III of the somatosensory cortex before and after cortical application of T-peptide (100 nM, 20 min) (Figure 1(a) to (d)). Under baseline conditions, *Cdh5*-GCaMP mice demonstrated endothelial Ca^{2+} activity throughout the FOV. Approximately 20 minutes after adding T-peptide to the cranial window, we observed a significant reduction in Ca^{2+} activity from baseline ($\sim 39\%$ reduction; 8423 ± 2284 vs. 3257 ± 1130 ZUMS; $n = 5$; $P < 0.05$)

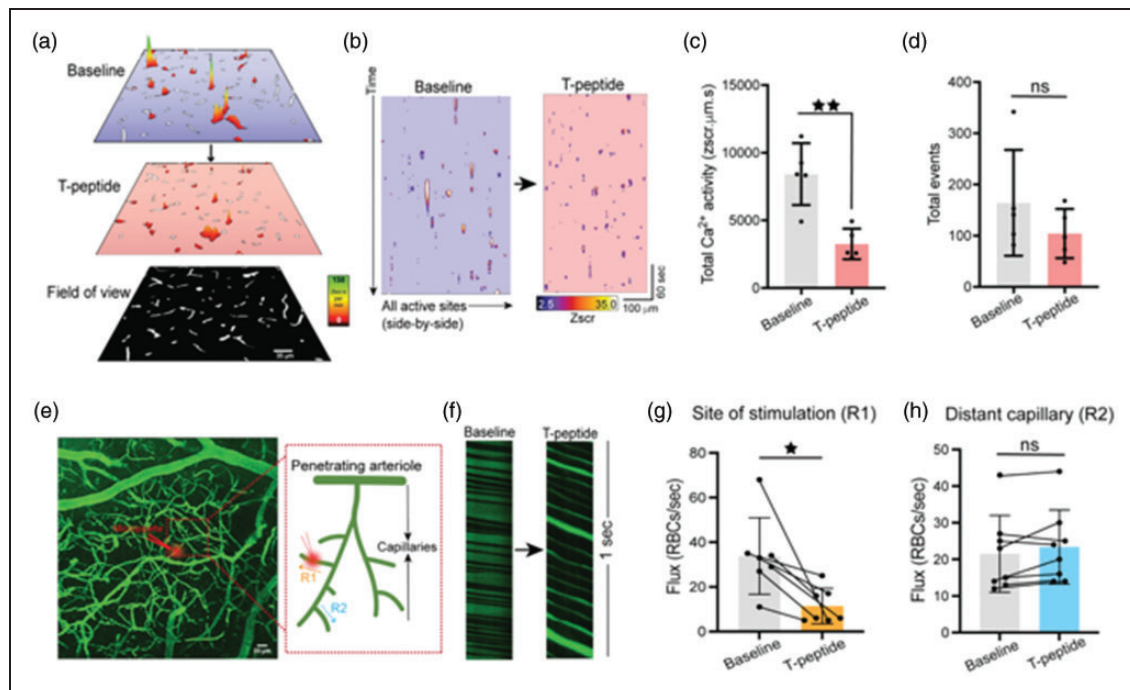


Figure 1. T-peptide significantly diminishes total Ca^{2+} activity in capillaries and regional RBC flux *in vivo*. (a) Prevalence maps from the same field of view showing total Ca^{2+} activity amplitude (Zscr.s) sites before and after exogenous application of T-peptide (100 nM) in *Cdh5*-GCaMP8 mice *in vivo*. Scale bar = $35 \mu\text{m}$. (b) Spatiotemporal (ST) maps of all individual active Ca^{2+} sites across the entire field of view before and after T-peptide exposure in *Cdh5*-GCaMP8 mice *in vivo*. (c) T-peptide significantly decreases total Ca^{2+} activity (39% reduction; 8423 ± 2284 vs 3257 ± 1130 ZUMS; $n = 4$ mice; $P < 0.05$; Paired *t*-test) but (d) not the number of total events (164 ± 103 vs 104 ± 48 # events; $n = 4$ mice; *n.s.*; Paired *t*-Test). (e) Micrograph of cortical vasculature. The red box denotes where subsequent capillary flow from mice at baseline and after T-peptide (100 nM) exposure was measured at the site of stimulation (R1) or connected distant capillary (R2) with a line scan. Scale bar = $20 \mu\text{m}$. (f) Representative line scan kymographs from a capillary showing the density and velocity of RBCs (black shadows interdigitated with labeled plasma (TRITC; green)) before and after pressure ejection of T-peptide (100 nm; 300 ms; 7 ± 1 psi) at the site of stimulation (R1). Note the reduced flow velocity and lower RBC flux after T-peptide application (right panel). Summary data showing and (g) significantly decreased RBC flux (34 ± 17 vs. 11 ± 8 RBCs/sec; $n = 4$ mice) after T-peptide exposure at site of stimulation (R1), $*P < 0.05$; Paired *t*-Test, but (H) not at the distant capillary (R2) (22 ± 10 vs. 23 ± 10 RBCs/sec; $n = 4$ mice), *ns*: not significant; Paired *t*-test.

(Figure 1(a) to (c)). Of note, T-peptide did not reduce the number overall active sites, determined by the count of Ca^{2+} events throughout the FOV during the recording period (# events, 164 ± 103 vs. 104 ± 48 ; $n = 5$; n.s.) (Figure 1(d)). This indicates that T-peptide decreases the Ca^{2+} output generated from individual active sites without impacting the number of sites themselves.

Next, we then measured RBC flux in 3rd–4th order capillaries in C57BL6/J mice injected with FITC-dextran (3 mg/mL, 150 KDa) for visualization of blood flow in the cortical vasculature. Low pressure ejection of T-peptide (100 nM; 300 msec; 6–8 PSI) resulted in a decrease in regional blood flow in 3rd–4th order branches of capillaries (R1) (Figure 1(e) to (g)). We observed a rapid reduction red blood cell (RBC) flux within 10–15 seconds of T-peptide exposure compared to baseline (Figure 1(g)), that persisted for the duration of the approximately 5 minute recording period (34 ± 17 vs. 11 ± 8 RBCs/s; $n = 4$ mice; $P < 0.05$).

This led to the question of whether reduction of RBC flux at the site of stimulation (R1) resulted in a redistribution of blood flow in connected branches of the capillaries. Thus, we measured RBC flux in capillary branches (R2), approximately 70 to 100 μm away from the target capillary R1 (Figure 1(e), inset). RBC flux measurements from the R2 region did not show a change (after T-peptide exposure to the R1 region) compared to the baseline (22 ± 10 vs. 23 ± 10 RBCs/s; $n = 4$ mice; n.s.) (Figure 1(h)). These data suggest that the changes in RBC flux are restricted to the site of T-peptide application and are not altered in the connected capillary branches during the time period of our observations.

T-peptide has endothelium-dependent vasoactive effects on cerebral arteries

We next tested the hypothesis that T-peptide impacts vasodilatory function in isolated pressurized pial arteries. Blood vessels were cannulated and allowed to develop myogenic tone at 80 mm Hg. Within 2 minutes of T-peptide (100 nM) application, vessels began to constrict. The endothelium-dependent vasodilator bradykinin was then used to test the effect of T-peptide on endogenous nitric oxide signaling. Bradykinin (10 μM) was administered before and 20 minutes after bath perfusion of T-peptide (100 nM). Time control experiments show that repeated application of bradykinin after 20 minutes produced a vasodilatory response that was not different from baseline (26 ± 8 vs. $21 \pm 3\%$ change in diameter; $n = 3$; n.s.). In contrast, after 20 minutes of T-peptide exposure, bradykinin-induced dilation was significantly attenuated (47 ± 31 vs. $12 \pm$

13% dilation before and after T-peptide respectively; $n = 7$; $P < 0.05$) (Figure 2(a) and (b)). T-peptide did not alter the response to the endothelial Ca^{2+} -activated K^+ channels, SK_{Ca} and IK_{Ca} , by NS309 (1 μM) (84 ± 19 vs. $67 \pm 32\%$ dilation; $n = 8$; n.s.) (Figure 2(c) and (d)). These results show that T-peptide specifically attenuated endothelium-dependent signaling mechanism(s), but the capacity for hyperpolarization-dependent vasodilation through Ca^{2+} -dependent activation of SK_{Ca} and IK_{Ca} channels remained intact. We further confirmed the effects of T-peptide are endothelial-specific, by testing the capacity of vascular smooth muscle to relax to the exogenous nitric oxide-donor spermine-NONOate in the presence of T-peptide. The concentration-response curve of spermine-NONOate (1–100 nM) was unaffected by T-peptide application (EC_{50} of control $-7.5 \mu\text{M}$ vs. T-peptide $-7.7 \mu\text{M}$; $n = 3$, n.s.) (Figure 2(e) and (f)). This indicates that T-peptide does not impair nitric oxide sensitivity in the vascular smooth muscle; instead, T-peptide acts directly on the endothelial cells to disrupt endothelium-dependent vasodilatory function.

Discussion

Tauopathy disrupts the targeted delivery of nutrients to active neurons in the brain through regional control of cerebral blood flow; this impairment in local functional hyperemia is an early manifestation of degenerative neurological diseases.^{6,7,18,19} Application of tau through a cranial window impairs local blood flow, reducing the endothelium-dependent vasodilation caused by acetylcholine.⁶ Similarly, mice with tauopathy produced through expression of aggregation-prone P301S-mutant human tau also exhibit impaired endothelium-dependent vasodilation *in vivo*.⁷ Administration of tau oligomer-specific monoclonal antibody (TOMA) rescued endothelium-dependent brain microvascular responses in this mouse model of tauopathy.⁷ Our results showing increased myogenic tone, impaired endothelium-dependent vasodilation, and reduced blood flow after T-peptide application are consistent with these prior reports. Together, these studies support a model in which tau protein accumulation in the brain leads to dysfunction of cerebral blood vessels, affecting their ability to regulate blood flow and maintain proper vascular tone. This dysfunction can impair blood flow to brain cells, limiting the delivery of oxygen and nutrients and the removal of waste products, thereby contributing to neurodegenerative processes.

Previously, the deranged cerebrovascular responses to tau were attributed to alterations in neuronal nitric oxide synthase (nNOS) and endothelial nitric oxide synthase (eNOS) function. In one study, it was shown that tau-induced dissociation of neuronal nitric oxide

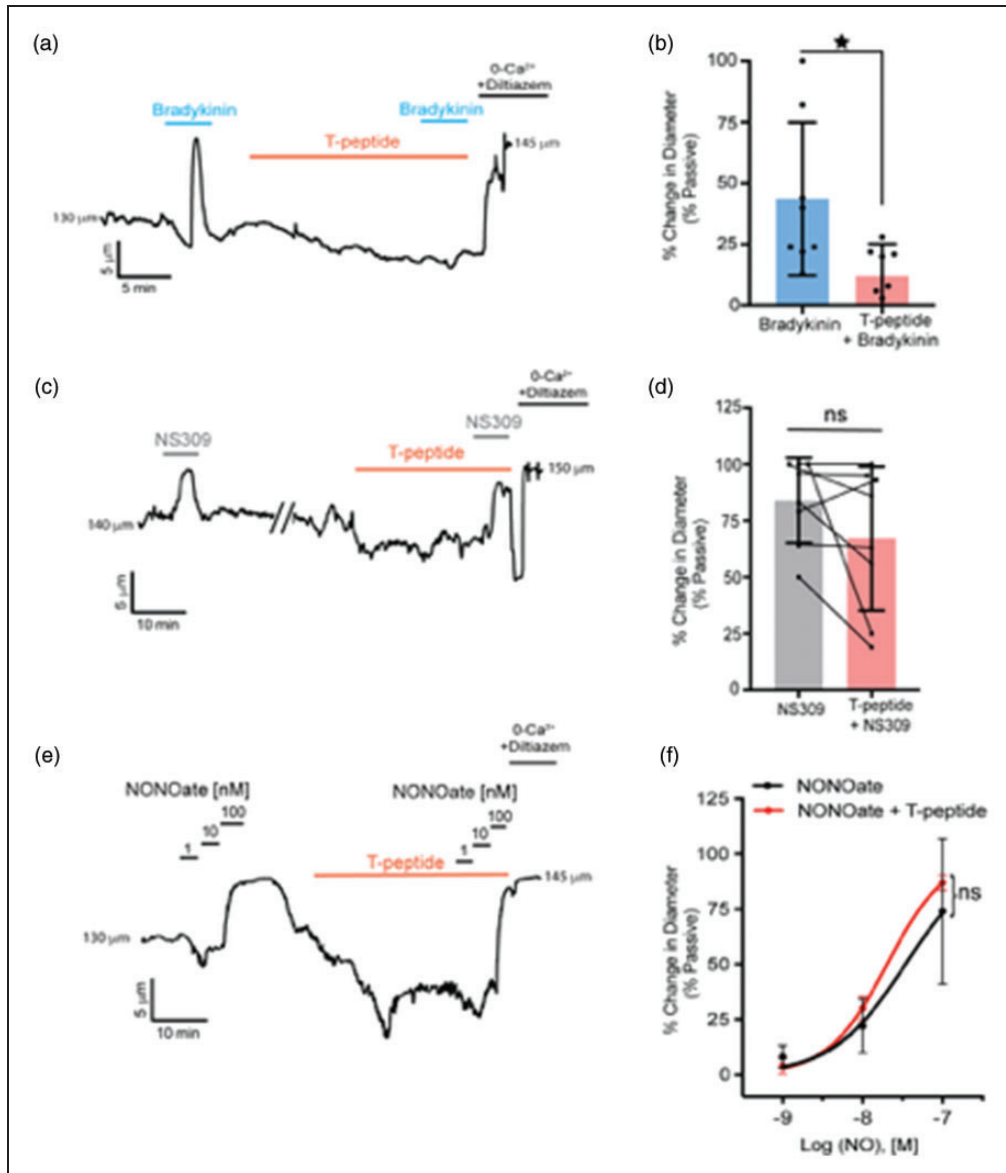


Figure 2. T-peptide diminishes bradykinin induced dilations but does not disrupt responsiveness to exogenous NO application. (a) Representative trace showing the response of a pressurized cerebral artery to exogenous application of bradykinin (10 μM), T-peptide (100 nM), and repeat bradykinin (10 μM) after 20 minutes of T-peptide exposure. (b) Summary data shows dilations to bradykinin (10 μM) were significantly diminished after T-peptide exposure (20 min; 100 nM) (47 ± 31 vs. $12 \pm 13\%$ change in diameter; $n = 8$ mice; $*P < 0.05$; *Unpaired t-test*). (c) Representative trace showing intact NS309 (1 μM) dilations before and after T-peptide exposure (20 min; 100 nM) in a pressurized cerebral artery. (d) Summary data shows NS309 (1 μM) dilations before and after exposure to T-peptide (100 nM) were not different (84 ± 19 vs. $67 \pm 32\%$ change in diameter; $n = 8$ mice; *n.s.*; *Paired t-test*). (e) Representative trace showing vasodilatory responses to increasing concentrations of the nitric oxide donor spermine-NONOate (1–100 nM) before and after T-peptide application (20 min; 100 nM) and (f) Summary data shows that T-peptide does not significantly diminish dilations to spermine-NONOate (1–100 nM) (LogEC₅₀ of control -7.5 ± 0.2 vs T-peptide -7.7 ± 0.04 μM; $n = 3$ mice; *n.s.*; *Ordinary two-way ANOVA*).

synthase (nNOS) from postsynaptic density 95 reduces nitric oxide production during glutamatergic synaptic activity, leading to failure of neurovascular coupling responses required for the regulation regional blood flow.⁶ In another study, it was reported that soluble pathogenic tau enters brain vascular endothelial

cells and drives cellular senescence with impaired cerebrovascular function. Specifically, cultured brain microvascular endothelial cells were shown to internalize soluble tau aggregates.⁷ The misfolded forms of tau protein contained in these aggregates promoted microtubule destabilization in cultured cells, as indicated by

reduced levels of acetyl-alpha-tubulin and overall microtubule density.⁷ This impaired the microtubule-dependent transport required for endothelial nitric oxide synthase (eNOS) translocation to the cell surface and subsequent nitric oxide production and induced cellular senescence. These competing models of tauopathy-induced cerebrovascular dysfunction are not mutually exclusive, however, cellular senescence would not explain the acute vasoconstriction or reduction in RBC flux and endothelium-dependent vasodilation that we and others have observed within minutes of application of tau to brain microvessels. Instead, we propose the novel concept that tau-induced microtubule reorganization disrupts the ability of endothelial cells to produce the Ca^{2+} signals needed for nitric oxide production and vasodilation. It has been well established that the microtubule cytoskeleton is needed for IP_3 -evoked Ca^{2+} signals in endothelial cells.^{9,10} Microtubules support the motility of IP_3 Rs, which is important because the diffusion and subsequent localization of the channel which is needed for efficient and graded recruitment of channels with increasing stimulus strength.¹¹ Microtubules interact with the TxIP motif of IP_3 Rs through the microtubule end-binding protein 3 (EB3), which is critical for clustering and functional coupling between IP_3 Rs.¹² Any effects on microtubule structure produced by soluble pathogenic tau aggregates would therefore be likely to influence IP_3 R-evoked Ca^{2+} signals. Moreover, a rise in cytosolic Ca^{2+} activates IP_3 Rs.^{20–22} Non-selective cation channels such as TRPV4,⁸ TRPA1²³ and Piezo1²⁴ are present in CNS capillary endothelial cells and are involved in the generation of capillary endothelial cells Ca^{2+} events. However, the extent to which tauopathy produces functional deficits of specific endothelial Ca^{2+} influx mechanisms are not yet known. These findings support our results showing that when T-peptide was applied directly to the brain vasculature of mice, can decrease in cerebrovascular endothelial Ca^{2+} activity.

This novel observation depended on the use of genetically encoded Ca^{2+} biosensor mice (*Cdh5-GCaMP8*) and advanced spatiotemporal mapping techniques to precisely quantify the mass of individual Ca^{2+} transients in brain capillary endothelial cells. The resulting statistical z-scores ($z_{\text{scr}}\text{-}\mu\text{m}\cdot\text{s}$) encompass the pixel intensity across the entire spatial area of an event over time. This provides reliable quantification of event amplitude for detection of even minute fluorescence changes with high reliability.⁸ Of note, T-peptide decreased the Ca^{2+} output generated from individual active sites without reducing the number of active sites themselves, suggesting a mechanism by which T-peptide possibly disrupts microtubule-dependent IP_3 R clustering needed to amplify local Ca^{2+} release events, which will be further tested in the future studies.

Furthermore, T-peptide application was associated with a significant reduction in local blood flow at the target capillary, but not in connected branches of the capillaries. Although, these measurements suggest that T-peptide induces a local reduction in the blood flow, simultaneous measurements of blood flow in multiple capillaries along arterioles and venules is needed to fully understand the cerebrovascular deficits produced by tau filaments.

Our findings are important because in Alzheimer's disease (AD), Chronic Traumatic Encephalopathy (CTE) and other degenerative neurological diseases, phosphorylated tau protein aggregates in cortical sulcus around small blood vessels.^{1–5} Tau is extruded to the extracellular space from damaged neurons where it oligomerizes in a process accelerated by tau phosphorylation. Pathogenic tau oligomers can transfer across synaptic clefts in brain circuits, to promote phosphorylation, misfolding and aggregation of native tau in adjacent cells through a prion-like process. This prion-like transmission through which tau proteins adopt pathogenic self-propagating conformations characteristic of prions has been well documented.^{25–27} Interestingly, it has been shown that lung microvascular endothelial cells themselves can release extracellular tau into the blood stream during bacterial pneumonia, causing cerebral tau aggregation and cognitive deficits.^{28,29} Of note, while the T-peptide portion of tau we utilized includes the C-terminal repeat region that is known to be important in tau aggregation, recent reports have demonstrated that mutations in the N-terminal region also impact the ability of tau to form larger-order complexes.³⁰ These findings warrant further effort to elucidate the potential vasoactive effects of tau protein in its full-length form, N-terminal region of Tau and also, in the presence and absence of post-translational modifications such as hyper-phosphorylation and acetylation that play a role in neurodegeneration.³¹ Moreover, tau prion strains differ in their ability to develop aggregates and toxicity in various brain regions.³² Because the extent to which different tau isoforms will produce cerebrovascular dysfunction may depend on their ability to form aggregates and/or induce toxicity, further evaluation of the effects of specific tau isoforms on the vascular functions of specific brain regions may be required to fully understand how tauopathy contributes to dementia.

In conclusion, our results support a novel paradigm in which tau accumulation contributes to abnormal cerebrovascular function through a mechanism specifically involving endothelial cells. We demonstrated that T-peptide reduces endothelial Ca^{2+} signaling, causes vasoconstriction, impairs endothelial-dependent vasodilation, and disrupts local cerebral blood flow. These

findings are significant because they support the strategy of protecting endothelial cells from tau to prevent the loss of cerebrovascular function in cognitive impairment and dementia.

Funding

The author(s) disclosed receipt of the following financial support for the research, authorship, and/or publication of this article: Research reported in this publication was supported by the National Institute of Aging (NIA) and National Institute of Neurological Disorders and Stroke (NINDS) (K99-AG-075175 to A.M.; R01-NS-110656, RF1-NS-128963-01 to M.T.N.; and R01-NS-119971 to Nikolaus Tsoukias, subcontract to M.T.N.), the National Institute of General Medical Sciences (NIGMS) (R35-GM-144099 to K.F. and P20-GM-135007 to M.T.N. and M.K.), the National Heart, Lung, and Blood Institute (NHLBI) (R35-HL-140027 to M.T.N. and R01 HL166944 to K.F.), the Department of Defense/The Henry M. Jackson Foundation for the Advancement of Military Medicine (HU001-18-2-0016 to W.L.), American Heart Association Career Development Award (856791 to A.M.), the Totman Medical Research Trust (to M.T.N.), the European Union Horizon 2020 Research and Innovation Programme (Grant Agreement 666881, SVDs@target to M.T.N.) and Leducq Foundation Transatlantic Network of Excellence (Stroke-IMPACT 19CVD01, to M.T.N.).

Declaration of conflicting interests

The author(s) declared no potential conflicts of interest with respect to the research, authorship, and/or publication of this article.

Authors' contributions

Conceptualization and experimental design A.M., A.M.S., K.F., M.K., G.B.; software analysis G.H., A.M.; data acquisition A.M., A.M.S., M.K., G.B., G.E.; data analysis A.M.S., A.M., G.H.; manuscript preparation and editing A.M.S., K.F., A.M., M.K., G.B., G.H., W.L., M.T.N.; project supervision and funding acquisition K.F., W.L., M.T.N.

References

- Shi Y, Zhang W, Yang Y, et al. Structure-based classification of tauopathies. *Nature* 2021; 598: 359–363.
- Vogel JW, Young AL, Oxtoby NP, et al. Four distinct trajectories of tau deposition identified in Alzheimer's disease. *Nat Med* 2021; 27: 871–881.
- Goldstein LE, Fisher AM, Tagge CA, et al. Chronic traumatic encephalopathy in blast-exposed military veterans and a blast neurotrauma mouse model. *Sci Transl Med* 2012; 4: 134ra60.
- McKee AC, Cairns NJ, Dickson DW, TBI/CTE group, et al. The first NINDS/NIBIB consensus meeting to define neuropathological criteria for the diagnosis of chronic traumatic encephalopathy. *Acta Neuropathol* 2016; 131: 75–86.
- Priemer DS, Iacono D, Rhodes CH, et al. Chronic traumatic encephalopathy in the brains of military personnel. *N Engl J Med* 2022; 386: 2169–2177.
- Park L, Hochrainer K, Hattori Y, et al. Tau induces PSD95–neuronal NOS uncoupling and neurovascular dysfunction independent of neurodegeneration. *Nat Neurosci* 2020; 23: 1079–1089.
- Hussong SA, Banh AQ, Van Skike CE, et al. Soluble pathogenic tau enters brain vascular endothelial cells and drives cellular senescence and brain microvascular dysfunction in a mouse model of tauopathy. *Nat Commun* 2023; 14: 2367.
- Longden TA, Mughal A, Hennig GW, et al. Local IP3 receptor-mediated Ca²⁺ signals compound to direct blood flow in brain capillaries. *Sci Adv* 2021; 7: eabh0101.
- Isshiki M, Ando J, Korenaga R, et al. Endothelial Ca²⁺ waves preferentially originate at specific loci in caveolin-rich cell edges. *Proc Natl Acad Sci U S A* 1998; 95: 5009–5014.
- Béliveau E and Guillemette G. Microfilament and microtubule assembly is required for the propagation of inositol trisphosphate receptor-induced Ca²⁺ waves in bovine aortic endothelial cells. *J Cell Biochem* 2009; 106: 344–352.
- Ferreri-Jacobia M, Mak D-OD and Foskett JK. Translational mobility of the type 3 inositol 1,4,5-trisphosphate receptor Ca²⁺ release channel in endoplasmic reticulum membrane. *J Biol Chem* 2005; 280: 3824–3831.
- Geyer M, Huang F, Sun Y, et al. Microtubule-Associated protein EB3 regulates IP3 receptor clustering and Ca⁽²⁺⁾ signaling in endothelial cells. *Cell Rep* 2015; 12: 79–89.
- Zhao K, Ippolito G, Wang L, et al. Neuron-selective toxicity of tau peptide in a cell culture model of neurodegenerative tauopathy: essential role for aggregation in neurotoxicity. *J Neurosci Res* 2010; 88: 3399–3413.
- Veloria JR, Li L, Breen GAM, et al. Novel cell model for tauopathy induced by a cell-permeable tau-related peptide. *ACS Chem Neurosci* 2017; 8: 2734–2745.
- Villalba N, Sonkusare SK, Longden TA, et al. Traumatic brain injury disrupts cerebrovascular tone through endothelial inducible nitric oxide synthase expression and nitric oxide gain of function. *J Am Heart Assoc* 2014; 3: e001474.
- Mughal A, Sackheim AM, Sancho M, et al. Impaired capillary-to-arteriolar electrical signaling after traumatic brain injury. *J Cereb Blood Flow Metab* 2020; 41: 1313–1327.
- Mughal A, Nelson MT and Hill-Eubanks D. The post-arteriole transitional zone: a specialized capillary region that regulates blood flow within the CNS microvasculature. *J Physiol* 2023; 601: 889–901.
- Austin SA and Katusic ZS. Loss of endothelial nitric oxide synthase promotes p25 generation and tau phosphorylation in a murine model of Alzheimer's disease. *Circ Res* 2016; 119: 1128–1134.
- Iadecola C. Untangling neurons with endothelial nitric oxide. *Circ Res* 2016; 119: 1052–1054.
- Clapham DE. Calcium signaling. *Cell* 2007; 131: 1047–1058.
- Foskett JK, White C, Cheung K-H, et al. Inositol trisphosphate receptor Ca²⁺ release channels. *Physiol Rev* 2007; 87: 593–658.

22. Arige V, Terry LE, Wagner LE, et al. Functional determination of calcium-binding sites required for the activation of inositol 1,4,5-trisphosphate receptors. *Proc Natl Acad Sci U S A* 2022; 119: e2209267119.
23. Thakore P, Alvarado MG, Ali S, et al. Brain endothelial cell TRPA1 channels initiate neurovascular coupling. *Elife* 2021; 10: e63040.
24. Harraz OF, Klug NR, Senatore AJ, et al. Piezo1 is a mechanosensor channel in central nervous system capillaries. *Circ Res* 2022; 130: 1531–1546.
25. Clavaguera F, Bolmont T, Crowther RA, et al. Transmission and spreading of tauopathy in transgenic mouse brain. *Nat Cell Biol* 2009; 11: 909–913.
26. Aoyagi A, Condello C, Stöhr J, et al. A β and tau prion-like activities decline with longevity in the Alzheimer's disease human brain. *Sci Transl Med* 2019; 11: eaat8462.
27. Condello C, Ayers JI, Dalgard CL, et al. Guam ALS-PDC is a distinct double-prion disorder featuring both tau and A β prions. *Proc Natl Acad Sci U S A* 2023; 120: e2220984120.
28. Balczon R, Lin MT, Lee JY, et al. Pneumonia initiates a tauopathy. *Faseb J* 2021; 35: e21807.
29. Choi C-S, Gwin M, Voth S, et al. Cytotoxic tau released from lung microvascular endothelial cells upon infection with *Pseudomonas aeruginosa* promotes neuronal tauopathy. *J Biol Chem* 2022; 298: 101482.
30. Cario A, Savastano A, Wood NB, et al. The pathogenic R5L mutation disrupts formation of tau complexes on the microtubule by altering local N-terminal structure. *Proc Natl Acad Sci U S A* 2022; 119: e2114215119.
31. Grundke-Iqbal I, Iqbal K, Tung YC, et al. Abnormal phosphorylation of the microtubule-associated protein tau (tau) in Alzheimer cytoskeletal pathology. *Proc Natl Acad Sci U S A* 1986; 83: 4913–4917.
32. Kaufman SK, Sanders DW, Thomas TL, et al. Tau prion strains dictate patterns of cell pathology, progression rate, and regional vulnerability in vivo. *Neuron* 2016; 92: 796–812.